JOURNAL OF GEOPHYSICAL RESEARCH, VOL. 104, NO. D16, PAGES 19,161–19,170, AUGUST 27, 1999

Assessment of smoke aerosol impact on surface solar irradiance measured in the Rondônia region of Brazil during Smoke, Clouds, and Radiation - Brazil

T. A. Tarasova,[1,2] C. A. Nobre,[1] B. N. Holben,[3] T. F. Eck,[4] and A. Setzer[5]

Abstract. The impact of smoke aerosols on the surface solar irradiance in the Rondônia region of Brazil is examined. The climate of this region is subequatorial with two distinct seasons. There is a sharp decline of the precipitation and cloudiness during the dry season which lasts from June to September accompanied by anthropogenic burning of savanna and forest in August and September with the resultant strong emission of smoke into the troposphere. Thus the magnitude of the column aerosol optical depth increases in these months while both precipitable water and cloud amount decrease in accordance with the seasonal cycle of humidity. All these atmospheric constituents influence the magnitude of the solar irradiance at the surface. In order to assess the aerosol and gaseous effects on the surface irradiance as compared with impact of cloudiness, we performed the clear-sky radiative transfer model calculations by employing a broadband radiation code and both aerosol optical depth and precipitable water retrieved from Sun photometer measurements. Calculation results show that the elevated aerosol optical depth observed in Rondônia during August and September causes a negative trend in the daily mean clear-sky surface solar irradiance during this period. Since the daily mean solar irradiance measured at the surface under all-sky conditions demonstrates a similar negative trend, it can be explained by the aerosol influence while the effect of clouds appears in the daily variations of the irradiance. It was also shown that smoke aerosols cause a decrease of the monthly mean values of all-sky surface irradiance in August and September as compared with July and October. Corresponding decreases in the near surface air temperature due to the smoke aerosols were not found.

1. Introduction

The state of Rondônia, Brazil, is located in the southern part of the Amazonia basin. It has a subequatorial climate characterized by high temperatures and humidities throughout the year. Nevertheless, seasonal variations of meteorological variables are observed on the ground as well as variations of water vapor amount, cloud amount, and aerosols in the atmosphere related to the change of the wet and dry seasons [*Gash et al.*, 1996]. The dry period is June to September, often with several weeks without rain, and the wettest period is December to April. The dominant vegetation of the Rondônia region is tropical rain forest. Progressive clearence related to agriculture results in biomass burning which occurs from August through September each year in the end of the dry season. Therefore a large amount of smoke aerosols is emitted into the troposphere during this period.

A large body of climatological data was obtained during the Anglo-Brazilian Climate Observational Study (ABRACOS) conducted in Amazonia from 1991 to 1993. In the Rondônia region, the measurements of the upward and downward radiative fluxes as well as meteorological variables were taken by automatic weather station at two observational sites established near Ji-Paraná. The climatological data of surface solar irradiance, humidity, and surface air temperature collected during ABRACOS from 1991 to 1993 are presented by *Culf et al.* [1996] without analysis of the main causes of seasonal variations of these variables. In this study we

[1]Centro de Previsão do Tempo e Estudos Climáticos/ Instituto National de Pesquisas Espaciais, Cachoeira Paulista, São Paulo, Brazil.

[2]On leave from Institute of Atmospheric Physics, Russian Academy of Sciences, Moscow.

[3]NASA Goddard Space Flight Center, Greenbelt, Maryland.

[4]Hughes STX Corporation, NASA Goddard Space Flight Center, Greenbelt, Maryland.

[5]Instituto Nacional de Pesquisas Espaciais, São Jose dos Campos, São Paulo, Brazil.

Paper number 1999JD900258.
0148-0227/99/1999JD900258$09.00

will investigate the data of surface solar irradiance and meteorological variables obtained at the ABRACOS site Reserva Jaru from 1992 to 1995. In order to estimate the effects of water vapor, ozone, and smoke aerosols on the clear-sky solar irradiance incoming at the surface, radiative transfer model calculations were performed by employing a broadband radiative transfer code and available data of aerosol optical depth and precipitable water obtained in August and September 1995 during the Smoke, Clouds, and Radiation - Brazil (SCAR-B) mission. The broadband radiation code developed for this study has the principal features of the shortwave radiative transfer codes employed in atmospheric general circulation models. The water vapor selective absorption, ozone continuum absorption, molecular scattering, and aerosol scattering and absorption are computed in 17 spectral intervals by using the Delta-Eddington method for the solution of the radiative transfer equation in 23 atmospheric layers. The daily and monthly mean values of clear-sky surface irradiance computed by the radiative transfer code were analyzed in conjunction with data obtained from continuous irradiance measurements at the Reserva Jaru site and in this way smoke aerosol effect on the all-sky irradiance was assessed.

Accurate calculations of surface radiative fluxes by atmospheric general circulation models are a prerequisite for adequate simulations of a regional climate. Nevertheless, recent studies indicate substantial uncertainties between measured and simulated solar irradiances at the Earth's surface [*Wild et al.*, 1995; *Le Roux et al.*, 1994]. The probable causes of these discrepancies are the deficiencies in the shortwave radiative transfer schemes, as well as the inaccurate simulation of the optical parameters of the atmosphere and cloud cover by the models. In order to study the accuracy of the shortwave radiative schemes under the clear-sky conditions, the comparisons were performed for the ground-based observations of the surface solar irradiance taken in conjunction with Sun photometer measurements [*Tarasova et al.*, 1992; *Kato et al.*, 1997]. It was shown that the difference can reach 40 $W m^{-2}$. Therefore further comparisons are required to estimate the accuracy of shortwave radiation codes in various atmospheric conditions. In this study, we compare the modeled and measured clear-sky surface irradiances using data sets obtained during SCAR-B at the observational sites of Cuiabá and Potosi Mine.

The observational sites Reserva Jaru, Cuiabá, Potosi Mine, and Ji-Paraná, where Sun photometer, pyranometer, and surface air temperature measurements were taken during SCAR-B are described in section 2 as well as instruments utilized for the measurements. Section 3 presents the annual cycle of cloudiness in the Rondônia region based on the satellite data as well as seasonal variations of meteorological variables obtained from the long-term measurements at the Reserva Jaru site. Section 4 describes the radiative transfer code developed and presents a comparison of the calculated and measured clear-sky surface irradiances at the Cuiabá and Potosi Mine sites. In section 5 we describe the daily and monthly mean values of the clear-sky surface irradiance at the Reserva Jaru site computed by the radiative transfer code and analyze them in conjunction with all-sky surface irradiance continuously measured at this site. The results and conclusions are discussed in section 6.

2. Description of Observational Sites and Instruments

Simultaneous measurements of the direct beam solar radiation and the broad band solar irradiance were taken in August and September 1995 at two observational sites, one in the Rondônia region: Potosi Mine (9°16′S, 62°52′W) and another in Mato Grosso: Cuiabá (15°30′S, 56°00′W). The direct beam solar radiation was measured every 15 min by a Cimel Sun photometer at the wavelengths 340, 380, 440, 500, 670, 870, 940, and 1020 nm [*Holben et al.*, 1996]. The derivation of the aerosol optical thickness at 500 nm was accurate to 0.02. The broadband solar irradiance measurements were taken at a 1 to 5 min sampling interval depending on the site [*Eck et al.*, 1998]. The total solar irradiance (285-2800 nm) was measured with Eppley precision spectral pyranometers, and photosynthetically active radiation (PAR) (400-700 nm) was measured with Skye-Probetech PAR Energy sensors (SKE-510). The errors in measured irradiance are estimated to be approximately 1.5-3.0% for both sensors [*Eck et al.*, 1998]. The Potosi Mine site is an abandoned tin mine, with only sparse vegetation and bare soil for a distance of at least 200 m from the instruments, and with dense forest surrounding the clearing of the mine site. The Sun photometer and pyranometer at the Potosi Mine site were located on top of a small hill within the cleared mine site, with an unobstructed horizon in all directions. The surface in Cuiabá is savanna with a mixture of buildings and parking lot in the immediate vicinity. The Sun photometer and pyranometers were located on the roof of one of the buildings of the Brazilian Instituto Nacional de Pesquisas Espaciais (INPE), affording a nearly unobstructed horizon in all directions.

Sun photometer measurements were taken also at the Ji-Paraná site (10°51′S, 61°47′W) by the Cimel Sun photometer mounted on the top of a water tower, about 25 m above ground level, on the immediate outskirts of the town, with the surface surrounding the site composed of a mixture of buildings, roads, and vegetation. The observations of the incoming solar radiation, net all-wave radiation, near surface air temperature, and humidity were conducted at the Reserva Jaru (10°05′S, 61°55′W) site of ABRACOS located about 80 km north of Ji-Paraná where the automatic weather station was mounted on the top of a 52 m tall tower, while the mean height of the forest canopy was 33 m. The total downward solar (300-3000 nm) and net

all-wave radiation were measured by CM-5 solarimeter (Kipp and Zonen, Delft, Netherlands) and by a single dome Q*6 radiometer (Radiation Energy Balance System , Seattle, Washington), respectively, at a 5 min sampling interval. The error in measured fluxes, which were recorded as hourly average data, is estimated to be about ±1% and ±3%, respectively. The near surface air temperature and dew point temperature were recorded every 10 minutes by wet and dry bulb platinum resistance thermometers (Didcot Instrument Company, Abington, England), and then averaged over 1 hour. These thermometers are accurate to ±0.1 °C. The water vapor pressure was calculated by using dew point temperature data [*Tetens*, 1930].

3. Background Climatology

The climate of the Rondônia region is characterized by a strong change of the monthly precipitation from 200 mm in April down to 5 mm in July [*Nobre et al.*, 1996]. The dry period is June to September when a corresponding decrease of the cloud cover and cloud water content also occurs. There are few ground-based observations of the cloudiness in Amazonia and central Brazil. Satellite observations from 1987 to 1988 over the Ji-Paraná region show that the monthly mean cloud cover changes from 80% in April to 15% in July, 25% in August, and 55% in September [*Rossow and Schiffer*, 1991]. The conventional visual observations at the airport in Porto Velho, located about 250 km northwest of Ji-Paraná, recorded scattered cloudiness of middle and high levels with cloud cover less than 50% from August 15 till September 15, 1995, during SCAR-B.

In order to describe background meteorological conditions in the Rondônia region, we computed monthly mean values of the radiative and meteorological variables, continuously measured at the Reserva Jaru site from 1992 to 1995, and averaged them over 4 years. The daily average solar irradiance incoming at the top of the atmosphere, S_{top}, and at the surface, S_i, is shown in Figure 1a, while Figure 1b presents daily minimum and daily maximum surface air temperatures, T_{min},T_{max}, and daily average water vapor pressure e. The values of S_{top} were calculated using the solar constant 1367 W m^{-2} [*Frohlich and London*, 1986]. The minimum of T_{min} and e occurs in July with 1 month delay compared to the minimum of S_{top} in June. The quite different annual cycle of the monthly mean daily maximum surface air temperature was found. The values of T_{max} increases from April to July, probably, due to increasing of S_i related to the decrease of cloudiness during dry season. The decreasing of the surface solar irradiance in August and September as compared with July and October is related to the smoke aerosol impact as shown in section 5. Note that the maximum temperature changes slightly in these months. Data obtained in 1995 are also shown in Figures 1a and 1b. As a result of lower cloud cover and lower rainfall, the higher temperatures

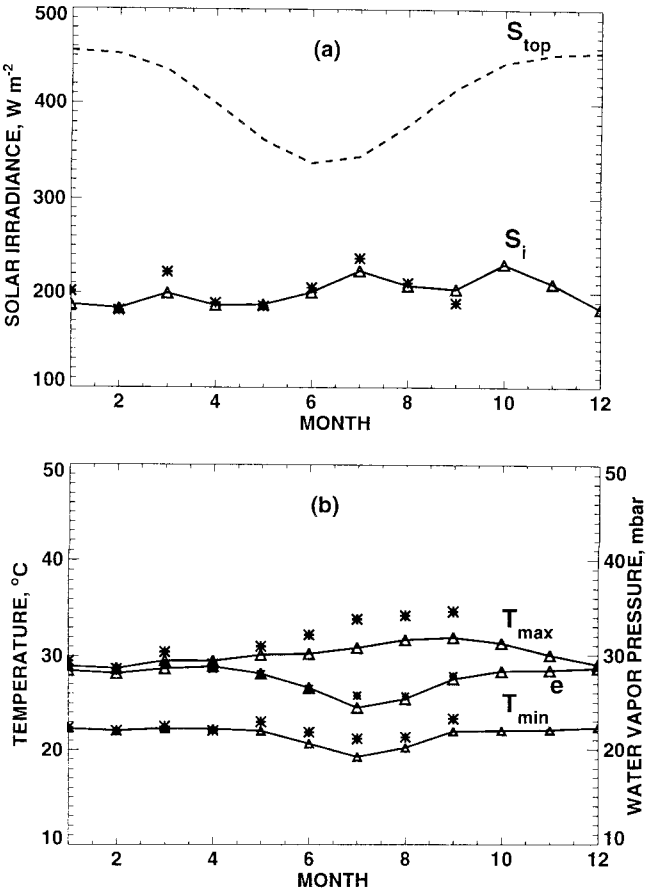

Figure 1. (a) Monthly mean values of incident solar irradiance computed at the top of the atmosphere, S_{top}, and measured at the surface at the Reserva Jaru (RJ) site, S_i. (b) Daily minimum and daily maximum surface air temperatures, T_{min},T_{max}, and daily average water vapor pressure e measured at RJ site. Asterisks, 1995 data; triangles, 1992-1995 averages.

compared to 4-year averages were observed from May to September 1995 which lead to the extensive biomass burning in that year.

4. Methodology for Computation of Solar Irradiance

The clear-sky radiative transfer model calculations were performed by the broadband radiative transfer code described in this section. Inputs in the code are the aerosol optical depth and precipitable water measured by Sun photometer. Optical and physical parameters of the atmosphere which were not available from the SCAR-B field measurements were obtained from standard atmospheric profiles of meteorological elements and aerosol models. Thus the aerosol single-scattering albedo ω_0 and asymmetry parameter g of the phase function of aerosol particles computed by Mie theory for three aerosol models were utilized. The values of these parameters in different spectral ranges are shown in Table 1. The continental aerosol model [*World Me-*

Table 1. Aerosol Single-Scattering Albedo ω_0 and Asymmetry Parameter g at Wavelength 0.5 μm and Also Averaged Over Three Near-Infrared Bands

	0.5 μm	0.7-1.22 μm	1.22-2.27 μm	2.27-5 μm
		Continental Aerosol Model		
ω_0	0.891	0.835	0.764	0.696
g	0.637	0.632	0.663	0.779
		Smoke Aerosol Model		
ω_0	0.866	0.813	0.722	0.588
g	0.623	0.609	0.603	0.631
		Stratospheric Aerosol Model		
ω_0	0.999	0.999	0.999	0.440
g	0.726	0.636	0.437	0.173

teorological Organization (WMO), 1986] consists of an in situ origin submicron mode (29% of the total volume), mineral coarse particle mode (70%), and a fine mode of soot (1%). The following average composition of smoke aerosols was obtained during SCAR-B [*Artaxo et al.*, 1996]: 71% submicron particles, 17% coarse particles, 7% oceanic particles, and 5% soot. We calculated the values of ω_0 and g for this smoke model also and used them in the tropospheric layers, while the stratospheric aerosol model [*WMO*, 1986] was incorporated in the stratosphere. Some numerical experiments were made with the continental aerosol model in the troposphere, as well as with the transformed smoke model, in which the aerosol single-scattering albedo at 550 nm was changed to $\omega_{550} = 0.95$ with the same shape of the spectra.

4.1. Broadband Radiative Transfer Code

The radiative transfer scheme is based on the vertically inhomogeneous Delta-Eddington technique [*Joseph et al.*, 1976]. Computations are carried out for 14 intervals in the visible and ultraviolet solar spectrum ($0.2\ \mu\text{m} < \lambda < 0.7\ \mu\text{m}$) and for three bands in the near infrared region: ($0.7\ \mu\text{m} < \lambda < 1.22\ \mu\text{m}$), ($1.22\ \mu\text{m} < \lambda < 2.27\ \mu\text{m}$), and ($2.27\ \mu\text{m} < \lambda < 5.0\ \mu\text{m}$). The upper boundary of the third band is 2.8 μm for the case of comparison with pyranometer measurements and is 10.0 μm in comparisons with line-by-line calculations. The molecular scattering, absorption, and scattering by aerosol particles, as well as the absorption by the water vapor and ozone are taken into account. In order to calculate the solar radiation absorption by water vapor in the scattering aerosol layer, the k-distribution method [*Wiskombe and Evans*, 1977] is utilized by incorporating the effective parameterizations for the k-distribution function presented by *Chou and Lee* [1996]. To compute the solar radiation absorption by ozone, the broadband absorption coefficients of O_3 prepared by *Briegleb* [1992] are adopted. In the computations of the integral solar irradiance, we use the extraterrestrial solar spectrum presented by *Frohlich and London* [1986].

4.2. Parameters of the Atmosphere and the Surface Adopted for Use in the Radiative Transfer Code

The following atmospheric parameters were adopted for use in the radiative transfer code from standard models. The vertical profile of the molecular scattering coefficient is computed by *Pendorf*'s [1957] formula. The height distribution of ozone amount is either tropical atmosphere profile or midlatitude summer profile [*McClatchey et al.*, 1972]. The normalized height distribution of the water vapor amount is one of two standard atmosphere profiles divided by its column water vapor amount. The normalized height distribution of the aerosol extinction coefficient in the boundary layer of the atmosphere is either convective (CONV) or continental (CONT-I) profiles [*WMO*, 1986] divided by the corresponding surface extinction coefficient ε_s. The aerosol extinction coefficient at 550 nm has exponential distribution with height in the lower 4 km atmospheric layer in the first case (CONV), $\varepsilon = \varepsilon_s \exp(-z/1.0)$, and it is constant in the lower 2 km layer in the second case (CONT-I), $\varepsilon = \varepsilon_s = 0.1\ \text{km}^{-1}$. The surface albedo over savanna and clearings were assumed to be 0.06 in the visible spectrum and 0.28 in the near infrared as well as 0.04 and 0.22, respectively, over the tropical forest. These values of surface albedo are presented by *Briegleb* [1992] for the medium/tall grassland and evergreen broadleaved forest. The corresponding integral surface albedo is in a good agreement with the data measured in Amazonia from 1991 to 1993 at the ABRACOS sites [*Culf et al.*, 1995]: 0.17 over the grassland and 0.14 over the forest in September.

4.3. Testing of the Radiative Transfer Code

The accuracy of the broadband radiation code can be estimated when compared to available reference calculations and observational data. Table 2 presents the solar radiation absorption by water vapor and ozone in the atmospheric column computed by the broadband radiative transfer code (BRTC) developed for the study and by two precise line-by-line (LBL) techniques [*Chou and Lee*, 1996; *Fomin and Gershanov*, 1996]. The LBL calculations of *Fomin and Gershanov* [1996] were performed for gaseous atmosphere with and without incorporating the models of continual absorption by water wapor [*Clough et al.*, 1989] as well as of CO_2 and O_2 absorption bands. The difference related to the water vapor continual absorption is about 10 W m^{-2} computed for midlatitude summer atmosphere at the solar zenith angle equal 30°. The difference is about 9 W m^{-2} due to both CO_2 and O_2 absorption. Also the additional water vapor selective absorption was about 5 W m^{-2} in the visible region of solar spectrum less than 0.7 μm. These fine effects were not incorporated in the broadband code. We are planning to include them in the next version of the code and also perform detailed comparisons with LBL calculations. On the other hand,

Table 2. Absorption of Solar Radiation in the Atmosphere-Surface System, at the Surface, and in the Atmosphere Column, Calculated for the Midlatitude Summer Atmosphere

Radiation Codes	Water Vapor 0.7-10.0 μm		Ozone + Rayleigh 0.2-0.7 μm	
	$\theta = 30°$	60°	30°	60°
	Atmosphere-Surface Absorption			
Chou and Lee [1996]	543.4	315.0	429.0	236.2
BRTC	544.8	316.0	424.5	234.0
	Surface Absorption			
Chou and Lee [1996]	369.4	202.3	394.5	211.4
BRTC	368.6	201.6	390.6	209.5
	Atmosphere Absorption			
Chou and Lee [1996]	174.0	112.7	34.5	24.8
BRTC	176.2	114.7	34.0	24.5
Fomin and Gershanov [1996]	177.1			
Fomin and Gershanov [1996][a]	187.8			

Units in $W\,m^{-2}$. The surface albedo is set to 0.2; θ is the solar zenith angle. BRTC, broadband radiative transfer code.
[a]The model of continual absorption by water vapor is incorporated.

models of continual absorption by water vapor, CO_2 and O_2 should be more thoroughly tested themselves.

At present, there are few line-by-line calculations of solar radiative fluxes in the scattering aerosol atmosphere with gaseous absorption. In order to prepare test cases for further comparisons, we performed computations for the tropical standard atmosphere running the broadband radiative transfer code two times, with and without aerosols. In the troposphere, the values of aerosol single-scattering albedo and asymmetry parameter as well as the normalized aerosol optical depth wavelength dependence are from the smoke aerosol model. Table 3 shows the solar radiation absorption by water vapor and ozone in the molecular scattering atmosphere in the first column. In the second column there is the change of absorption due to the background aerosols characterized by the following parameters: extinction coefficient at the surface $\varepsilon_s = 0.2$ km^{-1}, column optical thickness $\tau_{550} = 0.22$, and CONV profile of ε. Then ε_s was increased by 2, 4, and 8 times. With the increase of the aerosol extinction coefficient the solar radiation absorption increases in the atmosphere and decreases at the surface. The total effect is the decreasing of the absorption in the atmosphere-surface system. Almost the same values of the solar radiation absorption were obtained with another vertical profile, CONT-I, of the aerosol extinction coefficient for the same column aerosol optical thickness. The difference was less than 3 $W\,m^{-2}$. On the contrary, the profiles of the solar heating rate differ for CONT-I and CONV height distributions. In the first case the strongest heating rate is near the top of the 2 km aerosol layer, and in the second case it is near the surface.

Table 3. Absorption of Solar Radiation in the Tropical Atmosphere by Water Vapor and Ozone, and Change of Absorption due to the Smoke Aerosol Impact Computed With the Aerosol Optical Thicknesses $\tau_{550} = 0.22, 0.42, 0.81, 1.6$

θ	H_2O,O_3 Rayleigh	$\varepsilon_s = 0.2$ km^{-1} $\tau_{550} = 0.22$	$\varepsilon_s = 0.4$ km^{-1} $\tau_{550} = 0.42$	$\varepsilon_s = 0.8$ km^{-1} $\tau_{550} = 0.81$	$\varepsilon_s = 1.6$ km^{-1} $\tau_{550} = 1.60$
		Atmosphere-surface absorption			
30°	968.5	-0.1	-1.1	-3.1	-6.1
60°	547.2	-9.8	-16.2	-25.1	-34.1
		Surface Absorption			
30°	745.4	-32.5	-63.6	-123.7	-232.7
60°	401.7	-34.4	-62.3	-109.5	-180.3
		Atmosphere Absorption			
30°	223.1	+32.4	+62.5	+120.6	+226.6
60°	145.5	+24.6	+46.1	+84.4	+146.2

Units in $W\,m^{-2}$. Variable ε_s is surface aerosol extinction coefficient at 550 nm; θ is solar zenith angle; the surface albedo is set to 0.2.

Table 4. Six Time Periods During SCAR-B When the Measurements of Both Aerosol Optical Depth and Broadband Solar Irradiance Were Taken Under Cloudless Conditions

Period	Site	Date	Local Standard Time	$\bar{\tau}_{550}$	P_w
I	Cuiaba	Aug. 28, 1995	7 : 30 – 11 : 45	0.34	1.89
II	Cuiaba	Aug. 28, 1995	12 : 00 – 14 : 30	0.43	1.87
III	Cuiaba	Aug. 27, 1995	11 : 45 – 16 : 00	0.74	1.41
IV	Potosi Mine	Sep. 4, 1995	8 : 30 – 10 : 15	1.94	3.56
V	Potosi Mine	Sep. 4, 1995	9 : 00 – 10 : 45	2.14	4.13
VI	Potosi Mine	Sep. 4, 1995	11 : 00 – 12 : 00	2.46	4.30

Variable $\bar{\tau}_{550}$, column aerosol optical thickness at 550 nm; P_w, total precipitable water in centimeters.

Six time periods when Sun photometer and surface irradiance measurements have been taken under cloudless conditions at the Cuiabá and Potosi Mine sites were selected for the comparison of modeled and measured clear-sky surface solar irradiances. Table 4 presents the aerosol optical thickness $\bar{\tau}_{550}$ at the wavelength 550 nm and precipitable water P_w, obtained for each period. The values of τ_{550} were computed by interpolating the values of τ_{500} and τ_{670} derived from Sun photometer measurements at 500 and 670 nm, respectively. Precipitable water (P_w) was retrieved from Sun photometer measurements at 940 nm. Figure 2a shows the values of τ_{550} measured every 15 min, and Figure 2b presents its normalized wavelength dependence, τ_λ/τ_{550}, averaged for each period. There are the fairly good agreement between measured and modeled aerosol optical depth wavelength dependences in the visible range for both smoke and continental models. The photosynthetically active radiation ($0.4\ \mu\text{m} < \lambda < 0.7\ \mu\text{m}$) and total solar irradiance ($0.285\ \mu\text{m} < \lambda < 2.8\ \mu\text{m}$) also measured at the Cuiabá and Potosi Mine sites during these periods are shown in Figure 3 as a function of cosine of solar zenith angle.

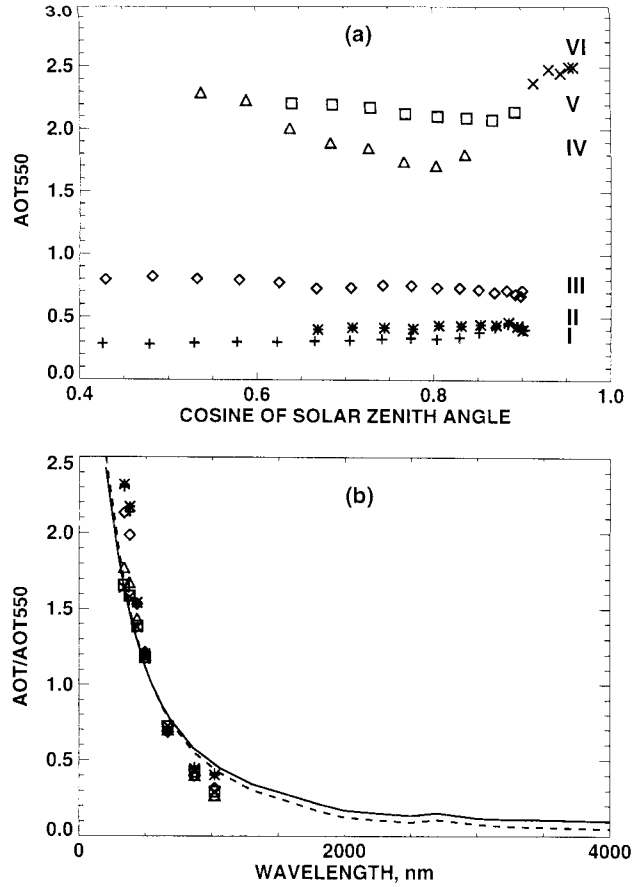

Figure 2. (a) Aerosol optical thickness at 550 nm (AOT550) measured by Sun photometer during six time periods shown in Table 4, and (b) the normalized wavelength dependence af aerosol optical depth, AOT/AOT550, averaged for each period; the solid curve presents AOT/AOT550 computed for continental aerosol model, and the dashed curve is for the smoke aerosol model.

The values of the aerosol optical depth and precipitable water obtained from sun photometer measurements taken every 15 min at the Cuiabá and Potosi Mine sites served as inputs in the radiative transfer code. Calculations were performed with either measured or modeled aerosol optical depth normalized wavelength dependence in the visible region. Note that there is no substantial difference between computed visible solar irradiances at the surface in these cases. Modeled aerosol optical depth wavelength dependence was used in the near infrared range due to the lack of sun photometer measurements at wavelengths greater than 1020 nm. Figure 3a shows the photosynthetically active radiation (PAR) computed by the code. For period I with aerosol optical depth $\bar{\tau}_{550} = 0.34$ the irradiances calculated with the smoke aerosol model ($\omega_{550} = 0.866$) as well as the continental model ($\omega_{550} = 0.891$) are in a good agreement with the measured data. The use of the smoke aerosol model in the computations instead of the continental model results in the smaller difference between measured and calculated PAR for period III with $\bar{\tau}_{550} = 0.744$. In order to obtain the good agreement for periods V and VI with very high aerosol optical depths $\bar{\tau}_{550} = 2.14, 2.46$, we used the transformed smoke aerosol model with the aerosol single-scattering albedo at 550 nm changed to $\omega_{550} = 0.95$ and with the same normalized wavelength dependence. The in-

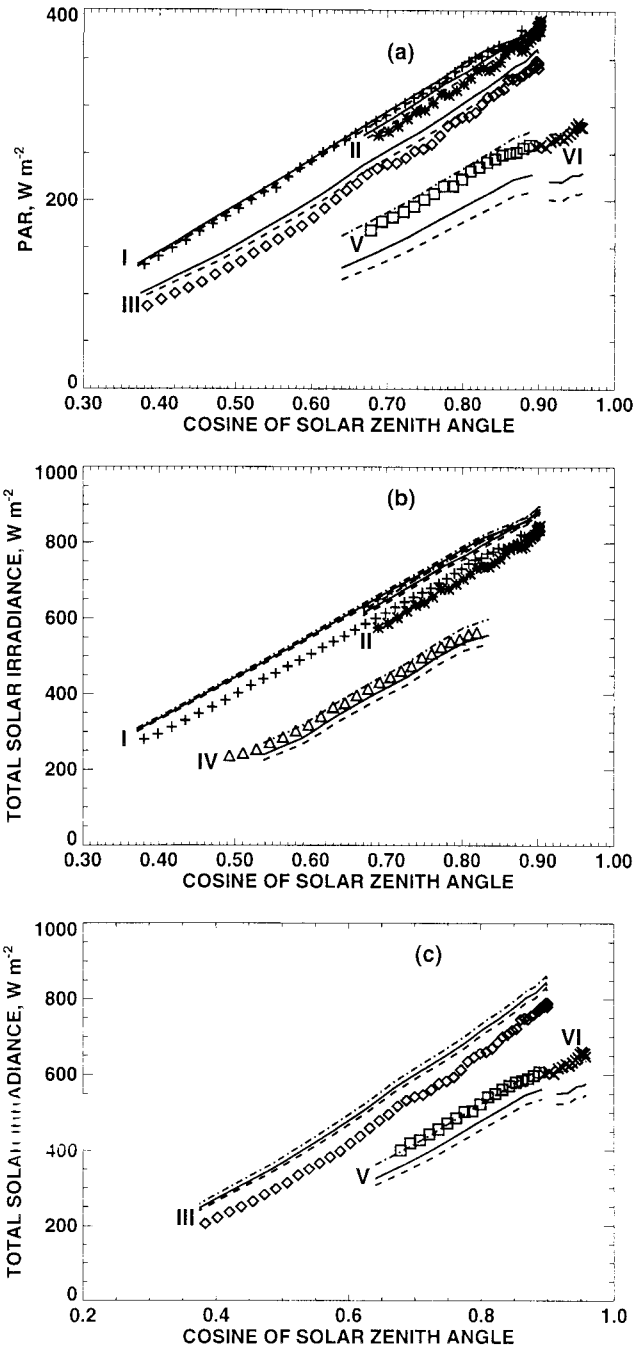

Figure 3. (a) Photosynthetically active radiation (PAR) and (b,c) total solar irradiance for six time periods shown in Table 4 and in Figure 2. Measured data are denoted by symbols, while the values computed with the continental aerosol model ($\omega_0^{550} = 0.89$) are denoted by solid curves, with smoke aerosol model($\omega_0^{550} = 0.87$) by dashed curves, and with $\omega_0^{550} = 0.95$ by dotted-dashed curves.

crease of the single-scattering albedo in heavy smoke hazes are caused, probably, by a combination of factors related to aging such as particle coagulation, gas to particle conversion, and cloud processing of aerosols. In addition, there is likely a higher fraction of smoldering phase combustion in Rondônia due to some forest burning compared to more flaming phase combustion in the savanna regions around Cuiabá.

Larger uncertainties were obtained between modeled and measured total solar irradiances. Figures 3b and 3c show that even for period I with small aerosol optical depth $\bar{\tau}_{550} = 0.34$ there is a difference from 20 to 40 W m^{-2} obtained with all the above mentioned aerosol models. This difference is caused, partially, by solar radiation absorption by CO_2, O_2, and water vapor continuum which is not incorporated in the code. Better agreement was obtained for periods IV,V,VI ($\bar{\tau}_{550} > 2.0$) when the transformed smoke aerosol model with $\omega_{550} = 0.95$ was utilized in the calculations. The difference between calculated and measured daily average total solar irradiances is 2 or 3 times smaller than the difference obtained at high solar zenith angles because it is computed by integrating instantaneous values over the day and then dividing by 24 hours. Therefore the accuracy of the calculations for daily average solar irradiance by this code should be less than 20 W m^{-2}.

5. Modeling of Gaseous and Aerosol Effects on Surface Irradiance

The values of daily average clear-sky solar irradiance at the surface were computed for 4 days in the beginning of August and for 16 days from mid-August to mid-September 1995 at the Reserva Jaru site. The nearest Sun photometer measurements were taken at the Ji-Paraná site located 80 km from Reserva Jaru. The aerosol optical depth $\bar{\tau}_{550}$ and precipitable water $\bar{P}_w$ derived from Sun photometer measurements served as inputs in the radiative transfer code. Figure 4 shows the daily average values of $\bar{\tau}_{550}$ and $\bar{P}_w$. The elevation of $\bar{\tau}_{550}$ after mid-August is related to an increase in biomass burning and a resultant larger smoke aerosol

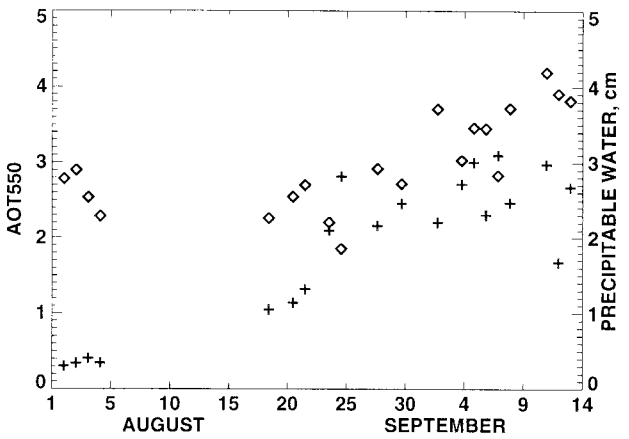

Figure 4. Daily average aerosol optical thickness at 550 nm (AOT550) (pluses), and precipitable water in centimeters (diamonds). Data were retrieved from Sun photometer measurements taken at the Ji-Paraná site during the first days of August 1994 and from mid-August to mid-September 1995.

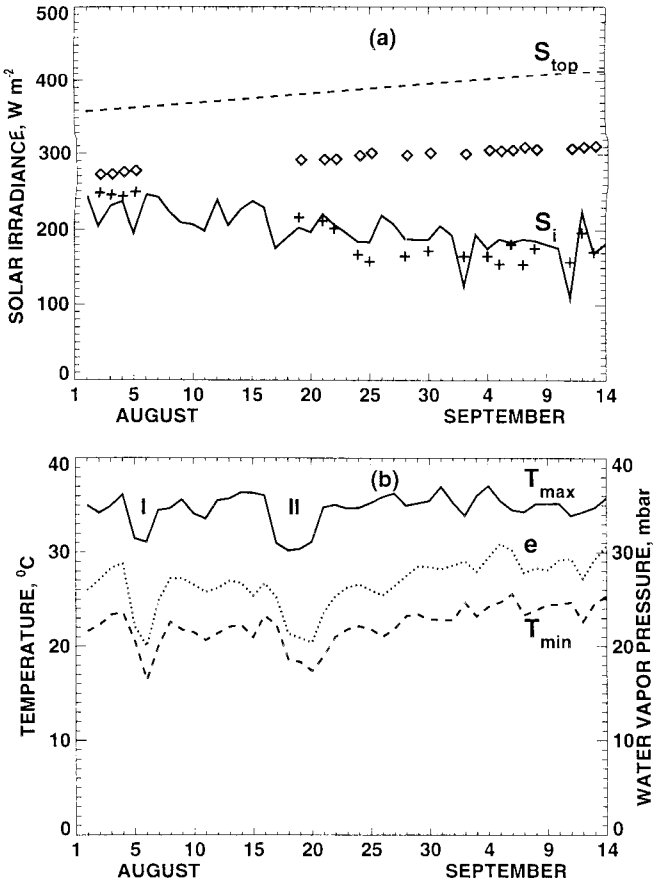

Figure 5. (a) Daily average incident solar irradiance S_i continuously measured at the Reserva Jaru site in August and September 1995, as well as computed at the top of the atmosphere S_{top} and at the surface for a gaseous cloudless atmosphere (diamonds) and gaseous cloudless atmosphere with aerosols (pluses). (b) Daily maximum and daily minimum surface air temperatures, T_{max},T_{min}, and daily average water vapor pressure e in millibars measured at the Reserva Jaru site.

emission while the growth of $\bar{P}_w$ is related to the main seasonal trend of humidity discussed in section 3. The magnitude of the aerosol optical thickness obtained in the beginning of August 1994 approaches the preburning period levels at this site [*Holben et al.*, 1996].

The radiative transfer code was run 2 times, with and without aerosols. The single-scattering albedo and asymmetry parameter of the smoke aerosol model were adopted by the code in the atmospheric layers below 12 km when $\bar{\tau}_{550} < 2.0$, while the aerosol single-scattering albedo at 550 nm was changed to $\bar{\omega}_{550} = 0.95$ when $\bar{\tau}_{550} > 2.0$ in accordance with the results described in section 4. Figure 5a shows the values of the daily average clear-sky solar irradiance computed by the code and measured under all-sky conditions, as well as solar radiative flux incoming at the top of the atmosphere. Solar irradiance at the top increases during this period due to the change of the astronomical position of the Sun-Earth relationship. Both water vapor and ozone attenuate the surface solar irradiance by the value that is in the range from 80 to 100 W m^{-2}, while the attenuation by aerosols is about 20 W m^{-2} in the beginning of August, and it is in the range from 70 to 150 W m^{-2} during the biomass burning period. The negative trend in the clear-sky solar irradiance is related to the smoke aerosol effect. Since an increase of cloud amount was not observed during this period, the negative trend in the observed all-sky solar irradiance can be explained by the aerosol impact. Cloudiness probably causes the daily variations of the irradiance. On September 6 a cloudless atmosphere was observed all day, and good agreement was obtained between calculated and measured total solar irradiances. The smaller values of calculated solar irradiance for the last days of August and first days of September, as compared with measured data, can possibly be explained by the overestimation of the daily average aerosol optical thicknesses at Reserva Jaru site by using data obtained at Ji-Paraná site. The cloud attenuation which can be approximately estimated from the difference of the computed clear-sky surface irradiance and irradiance measured under all-sky conditions is weak.

In order to reveal the possible aerosol impact on the daily variations of the meteorological variables, we considered the surface air temperature and water vapor pressure measured at the Reserva Jaru site from the beginning of August to mid-September 1995. The values of daily maximum and daily minimum surface air temperatures, as well as daily average water vapor pressure, for this period are shown in Figure 5b. The drop of both T_{max} and T_{min} during events I and II is caused by the advection of cold air from the south [*Marengo et al.*, 1997]. The positive trend in T_{min} and e from mid-August to mid-September is related to their annual cycle shown in Figure 1b. The only possible aerosol effect is in the absence of the positive trend in the daily maximum surface air temperature during this period.

We also calculated the monthly mean daily average clear-sky solar irradiances for 5 months from June to October at the Reserva Jaru site. The smoke aerosol model was adopted by the radiation code. The monthly mean aerosol optical thickness $\bar{\tau}_{550}$ and precipitable water $\bar{P}_w$ used in the calculations were retrieved from Sun photometer measurements taken at Ji-Paraná site from August to October 1995 and at the Alta Floresta site

Table 5. Monthly Mean Aerosol Optical Thickness $\bar{\tau}_{550}$ and Precipitable Water $\bar{P}_w$ Measured at Ji-Paraná Site in 1995 and at Alta Floresta Site in 1993

Month	τ_{550}	P_w, cm	Site
June	0.11	2.97	AF
July	0.16	2.88	AF
August	1.59	2.43	JP
September	1.71	3.65	JP
October	0.92	4.21	JP

JP, Ji-Paraná; AF, Alta Floresta.

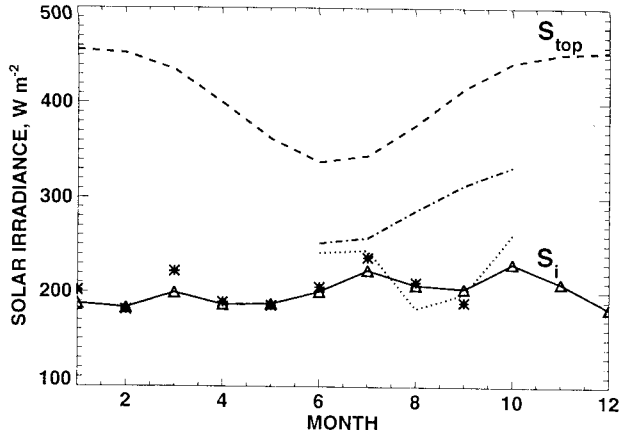

Figure 6. Monthly mean incident solar irradiance S_i measured at Reserva Jaru site in 1995 (asterisks) and from 1992 to 1995 (triangles), as well as incident solar irradiance calculated at the top of the atmosphere S_{top} and at the surface for a cloudless gaseous atmosphere (dotted-dashed) and for a cloudless gaseous atmosphere with aerosols (dotted).

during the preburning period in June and July 1993. Table 5 presents $\bar{\tau}_{550}$ and $\bar{P}_w$ data. The broadband radiation code was run 2 times. with and without aerosols. Figure 6 shows the calculation results. The attenuation of the incident solar irradiance by water vapor and ozone is in the range from 80 to 100 W m^{-2} for these months. The aerosols attenuate the solar irradiance by values range from 10 to 20 W m^{-2} in June and July, and from 100 to 110 W m^{-2} in August and September. The smaller values of the calculated solar irradiance for the clear-sky atmosphere in August, as compared with measured solar radiation under all-sky conditions, are, probably, related to the overestimation of the monthly mean daily average aerosol optical thickness at the Reserva Jaru site. The comparison of the clear-sky surface irradiance computed by the code and surface irradiance measured under all-sky conditions demonstrates that the decrease of both irradiances in August and September as compared with July and October is caused mainly by the smoke aerosol impact, while the effect of cloudiness is small. A decrease of the monthly mean daily maximum surface air temperature is not observed during these months, as is shown in Figure 1.

6. Results and Conclusions

The measurements of both aerosol optical depth and solar irradiance in August and September 1995 at observational sites in the Rondônia region and Mato Grosso provided data for the study of smoke aerosol impact on the incident solar radiative flux at the surface. A broadband radiative transfer code was developed and used for the analysis of the observational data. In order to test the radiative transfer code, we compared modeled and measured clear-sky solar irradiances for six time periods of radiation measurements taken under cloudless conditions at two sites, one in the Rondônia region and one in Mato Grosso. The average values of aerosol optical thickness obtained for these periods are τ_{550}=0.34, 0.43, 0.74, 1.94, 2.14, and 2.46, precipitable water changed from 1.89 to 4.3, and solar zenith angle varied from 16° to 68°. For period with small aerosol optical depth $\bar{\tau}_{550}$ = 0.34, the total solar irradiances calculated with the continental aerosol model as well as a smoke aerosol model overestimated measured data by the value that is in the range from 20 to 40 W m^{-2} or from 7 to 9%. This difference could not be eliminated by changing the aerosol single-scattering albedo at 550 nm since there was a good agreement between the calculated and measured values of photosynthetically active radiation (PAR) which differ less than 5 W m^{-2}. Possibly, changing the single-scattering albedo in the near infrared region may have resulted in better agreement with measurements. For high aerosol loading $\bar{\tau}_{550} > 2.0$ the solar irradiance computed with a continental aerosol model, $\omega_{550} = 0.89$, or with a smoke aerosol model, $\omega_{550} = 0.87$, underestimated measured solar irradiance by the values about 40 and 70 W m^{-2} or 7 and 17%, respectively, while use of the transformed smoke model with $\omega_{550} = 0.95$ in the calculations decreased this difference to less than 5 W m^{-2}.

To study the causes of these discrepancies further, detailed measurements of both aerosol size distribution, aerosol composition, and spectral aerosol optical properties should be held in conjunction with broadband radiation observations. Incorporating the models of continuum absorption by water vapor, CO_2, and O_2 as well as water vapor selective absorption in the visible spectrum in the radiative transfer code can lead to the decrease of PAR and total surface solar irradiance computed for a gaseous atmosphere without aerosols at high solar zenith angles by the values about 7 and 24 W m^{-2}, respectively. These effects in the aerosol laden atmosphere should be investigated more by means of precise radiative transfer calculations.

The impact of gases and aerosols on the daily average and monthly mean values of solar irradiance at the Reserva Jaru site measured under all-sky conditions were studied by comparing them with computed clear-sky surface irradiances. Calculations show that solar radiation attenuation by smoke aerosols cause a negative trend in the daily average clear-sky solar irradiance at the surface from the beginning of August to mid-September. The solar radiation absorption in the atmospheric column by smoke aerosols is comparable with absorption by water vapor, while the cloudiness effect for these dry season months with low cloud cover is much smaller. Therefore the decrease of the daily average all-sky solar irradiance observed during these months is also related to the increase of aerosol loading. The expected drop of the daily maximum surface air temperature was not found under the smoke hazes.

Possibly, the temperature effect of the aerosols is balanced by the increased solar radiation absorption in the boundary layer by absorbing aerosol particles versus reduced surface solar irradiance from both scattering and absorption effects. It was also shown by means of the clear-sky radiative transfer model calculations that the smaller monthly mean values of all-sky solar irradiance in August and September as compared to July and October are related to the larger smoke aerosol optical depths observed in August and September.

Acknowledgments. We thank all the people who helped to collect data used in the study. The presentation of the study was much improved due to the comments from the anonymous reviewers. One of the co authors (T. A. Tarasova) was supported by a CNPQ grant.

References

Artaxo, P., E.T. Fernandes, J.V. Martins, M.A. Yamasoe, K.M. Longo, P. Hobbs, and W. Maenhaut, Large scale elemental composition of atmospheric aerosols measured during SCAR-B, *in SCAR-B Proceedings*, pp. 9-14, Transtec, Sao Jose dos Campos, Sao Paulo, 1996.

Briegleb, B.P., Delta-Eddington approximation for solar radiation in the NCAR community climate model, *J. Geophys. Res., 97,* 7603-7612, 1992.

Chou, M.-D., and K.-T. Lee, Parameterizations for the absorption of solar radiation by water vapor and ozone *J. Atmos. Sci., 53,* 1203-1208, 1996.

Clough, S.A., F.X. Kneizys, and R.W. Davies, Line shape and the water vapor continuum, *Atmos. Res., 23,* 229-241, 1989.

Culf, A.D., G. Fisch, and M.G. Hodnett, The albedo of Amazonian forest and Ranchland, *J. Clim., 8,* 1544-1554, 1995.

Culf, A. D., J. L. Esteves, A. de O. Marques Filho, and H. R. da Rocha, Radiation, temperature and humidity over forest and pasture in Amazonia, *in Amazonian Deforestation and Climate,* edited by J.H.C. Gash et al., pp. 175-191, John Wiley, New York, 1996.

Eck, T.F., B.N. Holben, I. Slutsker, and A. Setzer, Measurements of irradiance attenuation and estimation of aerosol single scattering albedo for biomass burning aerosols in Amazonia, *J. Geophys. Res., , 103,* 31,865-31,878, 1998.

Fomin, B.A., and Y.V. Gershanov, Tables of the benchmark calculations of atmospheric fluxes for the ICRCCM test cases, II; Short-wave results, *Rep. IAE-5990/1,* 42 pp., Russian Res. Cent., Kurchatov Inst., Moscow, 1996.

Frohlich, C., and J. London (Eds.), *Revised Instruction Manual on Radiation Instruments and Measurements, WCR Publ. Ser.,* vol.7, 150 pp., World. Meteorol. Org., Geneva, 1986.

Gash, J.H.C., C.A. Nobre, J.M. Roberts, and R.L. Victoria (Eds.), An overview of ABRACOS, *in Amazonian Deforestation and Climate,* pp.1-14, John Wiley, New York, 1996.

Holben, B.N., A. Setzer, T.F. Eck, A. Pereira, and I. Slutsker, Effect of dry-season biomass burning on Amazon basin aerosol concentrations and optical properties, 1992-1994, *J. Geophys. Res., 101,* 19,465-19,481, 1996.

Joseph, J.H., W.J. Wiskombe, and W.A. Weinman, The Delta-Eddington approximation for radiative flux transfer, *J. Atmos. Sci., 33,* 2452-2459, 1976.

Kato, S., T.P. Ackerman, E.E. Clothiaux, J.H. Mather, G.G. Mace, M.L. Wesely, F. Murcray, and J. Michalsky, Uncertainties in modeled and measured clear-sky surface shortwave irradiances, *J. Geophys. Res., 102,* 25,881-25,898, 1997.

Le Roux, X., J. Polcher, G. Dedieu, J.C. Menaut, and B. Monteny, Radiation exchanges above West African moist savannas: Seasonal patterns and comparison with a GCM simulation, *J. Geophys. Res., 99,* 25,857-25,868, 1994.

Marengo, J., C. Nobre, and A. Culf, Climatic impacts of the "friagens" in forested and deforested areas of the Amazon Basin, *J. Appl. Meteor., 36,* 1553-1566, 1997.

McClatchey, R.A., R.W. Fenn, J.E.A. Selby, F.E. Volz, and J.S. Garing, Optical properties of the atmosphere, *Rep. AFCRL-72-0497, [NTISN 7318412],* 108 pp., Air Force Cambridge Res. Lab., Bedford, Mass., 1972.

Nobre, C.A., G. Fisch, H.R. da Rocha, R.F. da F. Lyra, E.P. da Rocha, A.C.L. da Costa, and V.N. Ubarana, Observations of the atmospheric boundary layer in Rondônia, *in Amazonian Deforestation and Climate,* edited by J.H.C. Gash et al., pp. 413-424, John Wiley, New York, 1996.

Pendorf, R., Tables of the refractive index for standard air and the Rayleigh scattering coefficient for the spectral region 0.2 and 20 mcm and their application to atmospheric optics, *J. Opt. Soc. Am., 47,* 176-182, 1957.

Rossow, W.B., and R.A. Schiffer, ISCCP cloud data products, *Bull. Am. Meteorol. Soc., 72,* 2-20, 1991.

Tarasova, T.A., G.M. Abakumova, and I.N. Plakhina, Determination of the absorbing properties of aerosol haze from measurements of direct and total solar radiation with a clear-sky, *Izv. Russ. Acad. Sci. Atmos. Oceanic Phys.,* Engl. Transl., *28,* 288-294, 1992.

Tetens, O., Uber cingie meteorologische Begriffe, *Z. Geophys., 6,* 297-309, 1930.

Wild, M., A. Ohmura, H. Gilden, and E. Roeckner, Regional climate simulation with a high resolution GCM: Surface radiative fluxes, *Clim. Dyn., 11,* 469-486, 1995.

Wiskombe, W.J., and J.W. Evans, Exponential-sum fitting of radiative transmission functions, *J. Comput. Phys., 24,* 416-444, 1977.

World Meteorological Organization, World Climate Research Programme: A preliminary cloudless standard atmosphere for radiation computation, *Rep. WCP-112, WMO/TD - No.24,* 53 pp., Geneva, 1986.

T. F. Eck, Hughes STX Corporation, Code 923, NASA Goddard Space Flight Center, Greenbelt, MD 20771. (tom@spamer.gsfc.nasa.gov)

B. N. Holben, NASA Goddard Space Flight Center, Code 923, Greenbelt, MD 20771. (brent@spamer.gsfc.nasa.gov)

C. A. Nobre and T. A. Tarasova, Centro de Previsão de Tempo e Estudos Climáticos/Instituto Nacional de Pesquisas Espaciais, Rodovia Presidente Dutra, km. 40, 12630-000, Cachoeira Paulista, São Paulo, Brazil. (nobre@cptec.inpe.br; tatiana@cptec.inpe.br)

A. Setzer, Instituto Nacional de Pesquisas Espaciais, São Jose dos Campos, São Paulo, Brazil. (asetzer@ltid.inpe.br)

(Received July 12, 1998; revised March 26, 1999; accepted March 26, 1999.)